Flume experiments on the impact of a cross-flow turbine on an erodible bed

Mohsen Ebrahimi*, Susannah Duncan, Michael R. Belmont, Prakash Kripakaran, Gavin Tabor, Ian Moon, Slobodan Djordjević

College of Engineering, Mathematics and Physical Sciences, University of Exeter, North Park Road, Exeter EX4 4QF, United Kingdom

ABSTRACT

Understanding the effect of tidal turbines on local erosion of the estuarine bed is crucial for design and maintenance of turbines with stable foundations and assessment of their environmental impacts. This report describes the results of flume experiments on clear-water scour caused by a single cross-flow turbine in steady flow conditions. The turbine investigated is a Momentum Reversal Lift (MRL) turbine originally designed in collaboration with the University of Exeter. Results show that the turbine can cause significant bed scour. particularly when it was not spinning and in a particular orientation of blades. This is opposite to the previous findings for axial flow turbines. The bottom plate of the turbine, although increasing scour depth, was found to increase the turbine performance and reduce adverse effects on the downstream flow. The findings highlight the importance of regular monitoring and taking immediate repair actions for a tidal installation.

Keywords: Flume experiments, scour, tidal turbine, cross-flow turbine

1. Introduction and background

Tidal energy has the potential to be a significant contribution to energy generation in the UK. In particular, significant amounts of energy can potentially be extracted from shallow-water estuarine zones which are abundant around the UK. This energy resource is predicted to represent nearly 50% of the tidal energy potential of the whole of Europe (Elghali et al. 2007; Magagna and Uihlein 2015) and, if realized, could save million tonnes of carbon annually and power millions homes. This energy can be extracted through barrages or through freestanding underwater hydrokinetic turbines, and there are significant reasons for preferring the latter. However the use of hydrokinetic turbines in practice is currently limited with an important factor being the challenge in evaluating their effects on seabed erosion, foundation stability and marine life. The importance of studying these effects therefore cannot be overestimated.

The Momentum Reversal Lift (MRL) turbine is a novel design of hydrokinetic turbine, originally designed by Aquascientific Ltd in collaboration with University of Exeter, UK. The flow hydrodynamics and power output of the MRL turbine have been studied both computationally and experimentally (Gebreslassie 2012; Gebreslassie et al. 2013a; b; Ordonez-Sanchez et al. 2017; Sutherland et al. 2018). Its cross-flow design is also particularly suitable to the shallow water environment in an estuary. These factors make it a good choice for investigating the scour induced by a tidal turbine. Moreover, unlike axial flow devices (e.g. Hill et al. 2014, Hill et al. 2016a, Hill et al. 2016b, and Musa et al. 2018a) for which scour and hydrodynamics have been studied in literature, no previous study has investigated the scour effects of cross-flow turbines.

* Mohsen.Ebrahimi@mottmac.com

The findings of this work are expected to inform expertise and guidelines (e.g. Musa et al. 2018b) for optimal design and maintenance of hydrokinetic tidal turbines, more efficient extraction of marine renewable energy in the UK, and improved management of environmental effects.

2. Experimental setup and methodology

Experiments were carried out in a horizontal 605mm wide (= B = width of approach flow), 10m long sediment recirculating flume at the University of Exeter. The flume is equipped with a traverse system (with a movement precision of 1 μm) for positioning instruments at specified x, y and z coordinates, where x, y and z refer to streamwise, spanwise and vertical directions. A side view of a typical experiment is shown in Fig. 1 where x = 0 is at the left edge of the vertical plate; y = 0 is at the centreline of the flume (positive toward left when looking downstream); and z = 0 is at the surface of the initial flat bed level at time t = 0.

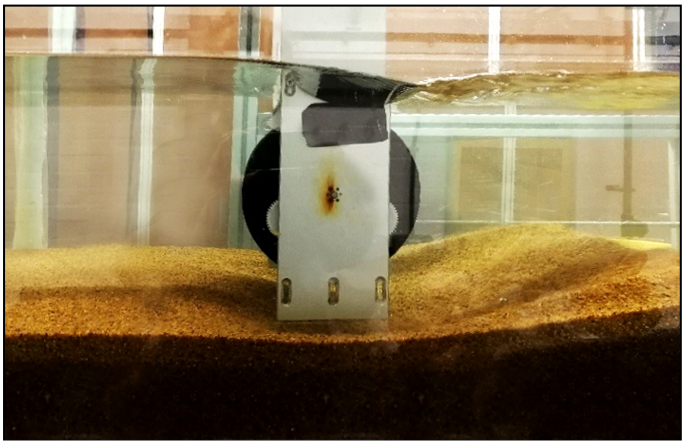

Fig. 1. Side view of the turbine in a preliminary experiment at t = 6 minutes. Flow is from left to right. Turbine is rotating clockwise.

2.1.Sediment

A difficult choice is the selection of particle size. The most common estuarine bed materials are alluvial muds. Unfortunately, their binding forces and bed flow processes depend on the absolute level of velocities and do not scale in any informative manner. Consequently, a uniform silica sand was chosen with a median particle size d_{50} = 1.37 mm which corresponds, at operation scale, to coarse gravel and thus has practical significance. This choice also accelerated scour process in the experiments. The chosen particle size resulted in clear-water scour conditions with U/U_{cr} = 0.93 where U is mean velocity of approach flow (= $Q/(Bh)$ where Q and h are flow discharge and depth of approach flow, respectively) and U_{cr} (= $U/\eta_*^{1/2}$, where η_* is relative flow intensity calculated according to Yalin and da Silva 2001) is critical velocity for initiation of sediment movement.

2.2. Turbine

The turbine used in the present work was a Momentum Reversal-Lift (MRL) turbine. A review of the turbine specifications is presented by Janssen and Belmont (2009), Ordonez-Sanchez et al. (2017) and Sutherland et al. (2018). The novelty of the MRL turbine is that it extracts energy by deploying both lift and momentum reversal (drag) of the flow on the turbine, thereby increasing power output. MRL turbine has three symmetrical blades rotating 180° for one full rotation of the primary shaft of the turbine. The high flow blockage ratio of the turbine makes it ideal for estuarine zones with shallow water. In practice, MRL turbines would be operated in extended horizontal arrays; so the use of a relatively narrow flume, with narrow wall layers (i.e. small gradient of streamwise velocity near the walls), does not constitute an unacceptable artefact. To minimize adverse effects, the original model was altered, as shown in Fig. 2, by removing its supports which were solely for structural integrity of the turbine.

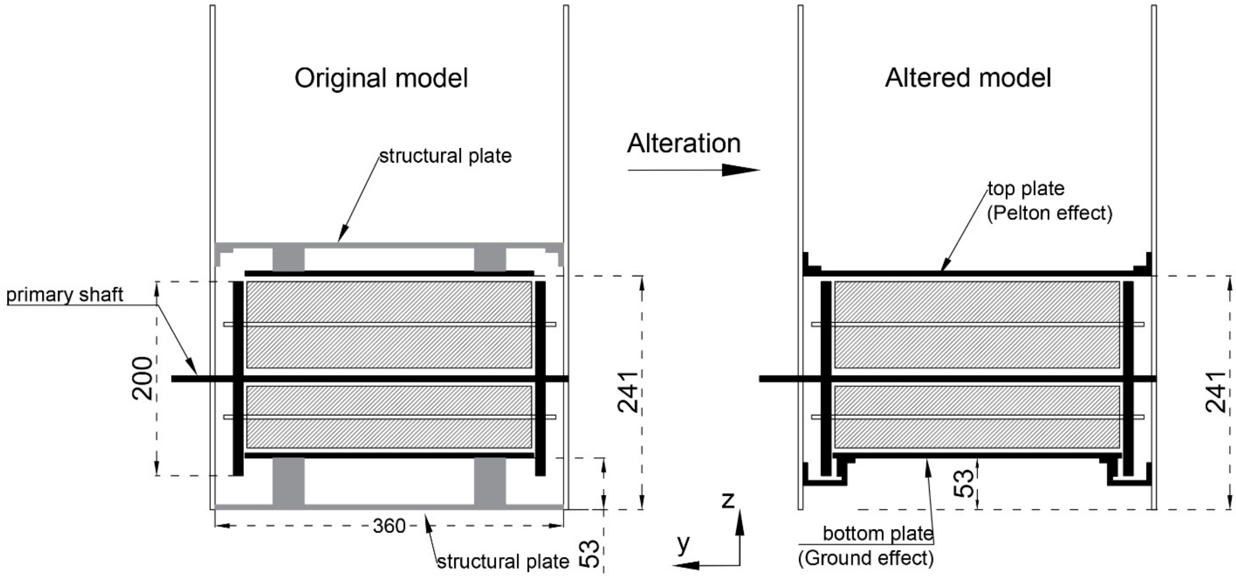

Fig. 2. Looking-downstream schematics of original (left) and altered (right) turbine models. Dimensions are in mm.

2.3. Hydraulic conditions of experiments

Four clear-water scour experiments were carried out with hydraulic conditions presented in Table 1. Here, R = flow Reynolds number (= Uh/v, with v being fluid kinematic viscosity); F = Froude number (= $U/(gh)^{1/2}$, where g stands for acceleration due to gravity); d_s is the maximum measured scour depth; and x_s = longitudinal coordinates of the maximum scour depth. Reynolds number was kept within the turbulent flow regime (R > 2000-3000, Chanson 2004) rather than ensuring strict similitude between the model and the prototype. Froude number was similarly kept within the subcritical regime (F < 1). Two rotation cases were examined; with the turbine fixed (non-rotating) and with it allowed to freely rotate. In the latter case, the turbine rotation speed is determined by a balance of the hydrodynamic forces with the frictional forces in the bearing, and therefore alters according to the hydrodynamic forces both between and during the experiments (as scour affects the hydrodynamic flow).

Table 1. Maximum scour depth measured in the present experiments

Run[a]	Description	h (± 1 mm)	Q (±0.1 L/s)	R	F	U/U_{cr}	d_s (mm)	x_s (mm)
H1	With bottom plate (40 mm from bed)	260	70	115702	0.28	0.93	95.7	376
H2	Without bottom plate						69.7	519
H3	Stationary blades without bottom plate						> 150[b]	~ 410[b]
P1	Without bottom plate						80.4	600

[a] H and P experiments were carried out with turbine hanging from above (representing floating turbine) and turbine mounted on piers buried in sand bed, respectively. In all experiments vertical elevation of the turbine was identical to test H1.
[b] scour reached flume bed and x_s is approximated value of location of maximum scour depth if bed thickness was not finite.

A schematic and photo of the looking-downstream cross section of the experiments are shown in Fig. 3. Two sets of experiments were carried out: 1) H Runs with turbine hanging from above (representing floating turbine) without extended side piers and 2) P Runs with the turbine being secured by extending its side piers into the sand and all the way to the flume bed (representing installation on piers). In all experiments, the turbine was installed at an elevation so that the bottom plate of the turbine was 40 mm from the bed. This elevation was chosen to maximise the scour seen during the experiment. To investigate the impact of the bottom plate, this was removed from certain runs as shown in Table 1.

The flow depth was identified as h = 260 mm to generate the maximum, streamwise, flow velocity (shown by the enhanced dot in Fig. 3) at the centre of the upper blade of the turbine. This was expected to be 89 mm from the free surface due to the dip phenomenon (Wang et al. 2001), where the maximum velocity occurs at a location below the free surface for cases with small aspect ratio B/h.

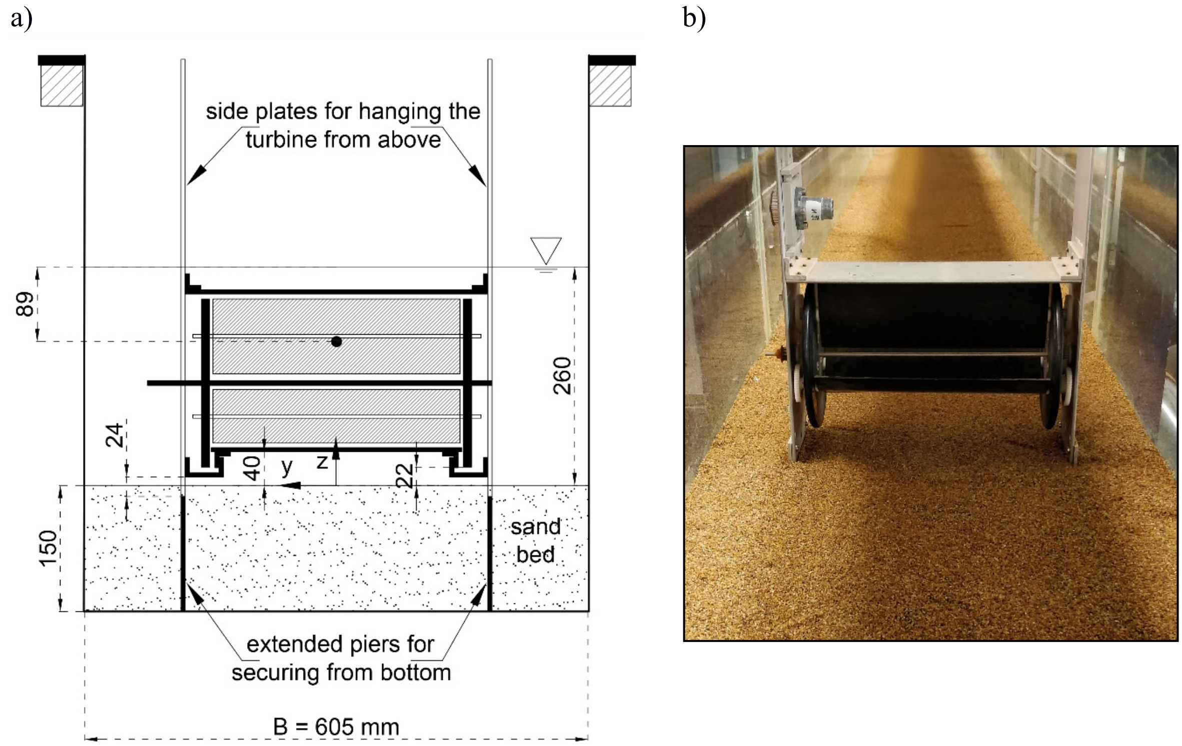

Fig. 3. Looking-downstream, cross-sectional schematic (left) and photo (right) of Run P1. The turbine was installed in two ways: 1) H Runs with turbine hanging from above (representing floating turbine) without extended side piers and 2) P Run secured by extended black plates buried in the bed. Enhance dot shows elevation of flow maximum velocity due to dip phenomenon (Wang et al. 2001).

Each experiment lasted 300 minutes at U/U_{cr} = 0.93. Although this duration was not sufficient to reach equilibrium scour depth, it was deemed acceptable to investigate the overall effect of turbine and its bottom plate on bed erosion. In Fig. 4, temporal variation of scour depth is shown in experiment P1 near the location of maximum scour downstream the turbine.

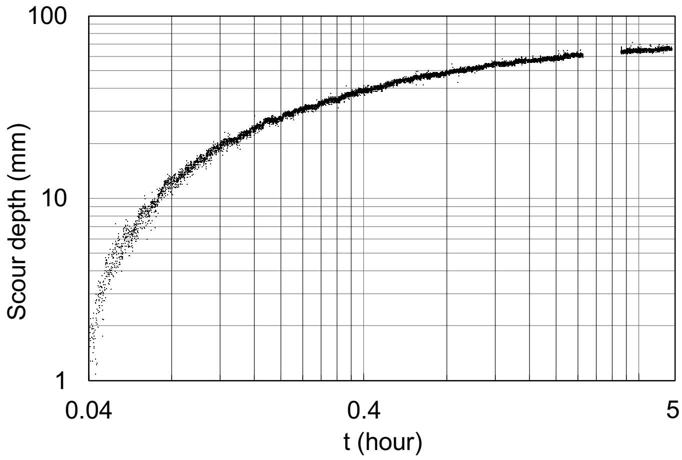

Fig. 4. Temporal variation of scour depth near the location of maximum scour depth in Run P1

3. Measurements

3.1. Flow discharge and free surface

Flow discharge was set by using a variable-speed drive on a centrifugal pump driving the flow. It was measured using an electromagnetic flowmeter (resolution ±0.1 L/s) installed in the suction pipe of the water recirculating system. A digital point gauge was used to read the elevation of free surface at the centreline of the flume. The precision of this measurement was ±0.5 mm due to free surface fluctuations.

3.2. Scour

In each scour experiment, the final scour topography (after 300 minutes) was mapped using an echo sounder. This was carried out in still water conditions after stopping the flow very gradually and removing the turbine. Scour topography was mapped by measuring distances from the bed on a grid of approximately 150 (x, y) points. The echo sounder utilised was one built into a Nortek Vectrino Profiler mounted on the traverse system of the flume. In this study, the Vectrino Profiler was used solely to measure bed topography; velocity profiles were not measured. The echo sounder used the time of flight of an acoustic signal to measure the distance to the bed and had an advertised accuracy of ±0.5 mm. To improve the spatial resolution, additional manual measurements were taken at $x = x_s$ and at the upstream end of the scour hole. This was carried out with a precision of ±0.5 mm using the digital point gauge after slowly draining the flume. Measurements were generally only taken on one side of the flume due to the observed symmetry in the scour profile about the x-z plane. This symmetry was confirmed for Run H2 using scour measurements taken on both sides of the flume. The repeatability of the experiments was confirmed by comparing the maximum scour depth and overall scour pattern obtained after 300 minutes over two repetitions for a couple of scenarios. A final map of the scour was produced to a conservative accuracy of ±2 mm by combining all the measured points.

3.3. Turbine revolution

In Runs H1 and H2, the temporal variation of the turbine rotation speed caused by the impact of the evolving scour pit on the hydrodynamics of the turbine was investigated. This was carried out by measuring the speed of the turbine rotation by video recording at t = 0, 6, 12, 18 and 295 minutes.

4. Results

4.1. Scour depth

Fig. 5 illustrates scour maps, between y = -190 and 190 mm, measured at t = 300 minutes. The maximum scour depth d_s was located downstream of the turbine anywhere between x = 300 ~ 600 mm. The eroded material was deposited further downstream at x = 1500 ~ 4000 mm in the form of a 4.5 ~ 7cm-height dune which is not recorded here. This large dune started developing at the onset of each experiment from the accumulation of eroded sand on the bed and could affect downstream environment and navigation if reproduced for a real installation. As shown in the figure, the bed significantly upstream of the turbine is not disturbed. This is due to the clear-water scour conditions in the experiments. The turbine obstructs the flow and diverts it toward the bed thereby causing significant scour downstream of the installation.

The first main observation is that the turbine caused significant erosion. This is presumed to be due to the large cross-sectional blockage, being ~ 35% of cross-sectional area, at t = 0, of the approach flow. By assuming an average scour depth of 100 mm after 300 minutes, the blockage ratio is estimated to decrease to ~ 29% due to scour evolution. The exact values of maximum scour depth d_s are summarised in Table 1. The largest scour depth among four experiments, occurred for Run H3 where the turbine blades were stationary and not spinning. The next greatest scour depths were for Run H1 with bottom plate, Run P1 with extended legs and Run H2 without the bottom plate. Removing the bottom plate in Run H2 caused the maximum scour depth to decrease by 28% compared to Run H1. In Run H1, the bottom plate split the flow into two parts, i.e. the flow over the plate and the accelerated flow beneath the plate, which separately rotated the turbine and eroded the bed, respectively. In Run H2, however, the flow is not split and its entire momentum is used to rotate the turbine as well as erode the bed. In Run H3, however, the turbine was still with a particular orientation of blades that caused a large obstruction to the flow and directed the flow energy toward the sand bed (see Fig. 6). This explains the larger scour depth in Run H3. In fact, the largest difference in maximum scour depth, of over 80 mm, was between Runs H2 and H3. It must be emphasized that an orientation of the turbine blades that is different to the one shown in Fig. 6 and poses a much smaller obstruction to the flow, may lead to significantly reduced scour. This highlights the importance of continuously monitoring the turbine operation since excessive scour may result depending on the position in which the turbine stopped working.

What is notable in Run P1, was local scour occurring around each of extended side piers of the turbine which was ~ 7 mm deeper than scour downstream of the turbine. This also highlights the importance of regular monitoring of bed status at the legs when the turbine is installed on buried legs. The aforementioned scour made Run P1 stand out from the other three experiments. In addition, side legs appear to have constricted the flow further toward the middle of the channel and slightly increased scour depth.

Further in this work, the local scour at the legs was excluded from the analysis to facilitate the comparison with the other experiments.

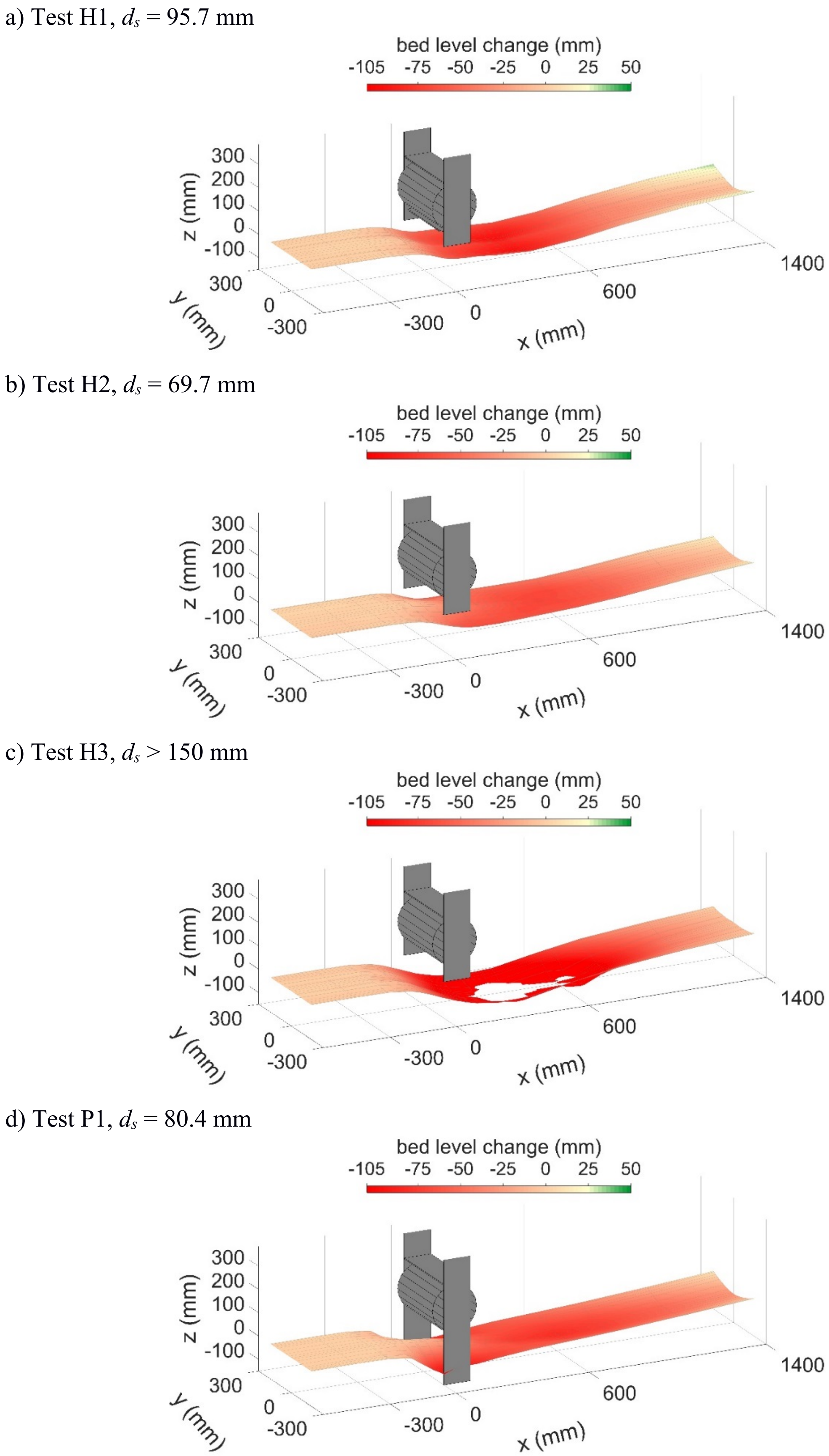

Fig. 5. Scour maps measured after 300 minutes

4.2. *Scour longitudinal profile and extent*

Fig. 6 illustrates longitudinal profiles of the bed topography along the centreline (CL) of the flume, i.e. at $y = 0$. For Run H1 an additional profile is shown at $y = -82$ mm (i.e. to the right of the centreline) which serves to point out the minor asymmetry of the bed topography. As seen earlier in Fig. 5, maximum scour depth is observed for Run H3 with the shown orientation of stationary blades. In this experiment, erosion reached the flume steel bed at about $t = 3$ hours. The exact value of the longitudinal coordinate of the maximum scour depth is presented in Table 1. In Run H1, maximum scour was observed closer to the turbine than in Runs H2 and P1. This can be explained by the presence of the bottom plate in Run H1 which channelled the flow towards the bed, while Runs H2 and P1 had no bottom plate to direct the flow downward. This made the scour profile shallower but longer in Runs H2 and P1 compared to Runs 1 and 3.

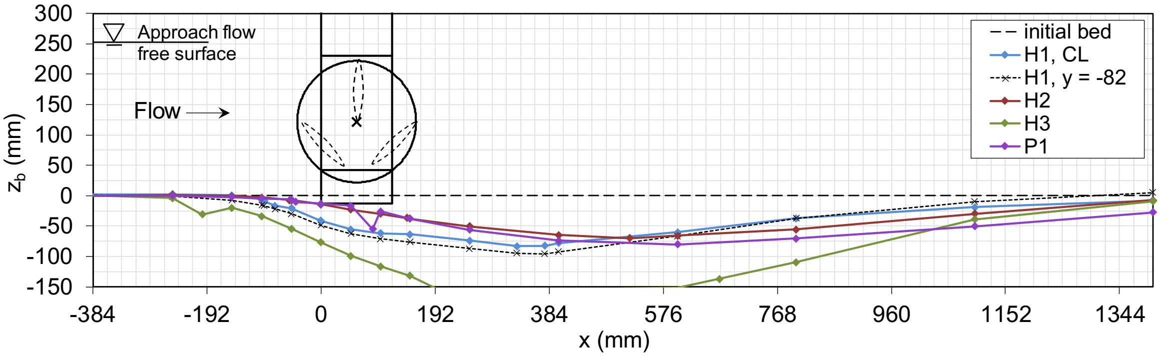

Fig. 6. Longitudinal scour profiles measured at centreline (CL) and y = -82 mm. Orientation of the blades at $t = 0$ is shown in the turbine circular disk.

4.3. Free surface profile

Fig. 7 shows variation of the elevation of the flow free surface, at the centreline, along the flume (except for Run P1 where the measurements downstream of the turbine were not available). This is presented in the form of differences of elevation relative to the elevation of the approach flow. The measured values are estimated to be accurate to within ±1 mm. The location of the turbine is represented by the black vertical rectangle with the flow being from left to right. As shown, changes in the free surface profile follow a similar trend for all four runs. There is a free surface rise immediately upstream of the turbine followed by a sudden and notable drop just beyond the turbine downstream. Afterwards, the free surface would start to regain some of its approach elevation, but due to the limited length of the flume it was not possible to determine whether it would ever fully attain its initial elevation. The free surface drop was largest in Run H3 because of the orientation of the stationary blades of the turbine which caused a larger acceleration to the flow. In Run H1 with bottom plate, the free surface rise and drop-off were smallest. This agrees with Gebreslassie (2012) who found that the bottom plate reduces free surface disturbances in the wake region of the turbine. For Run H2, approximate measurements suggested a profile shown by the dashed line which is between those of Runs H1 and H3. This implies a smaller adverse effect of the turbine on downstream flow compared to Run H3. For Run P1, the free surface profile downstream of the turbine is expected to be closest to Run H2.

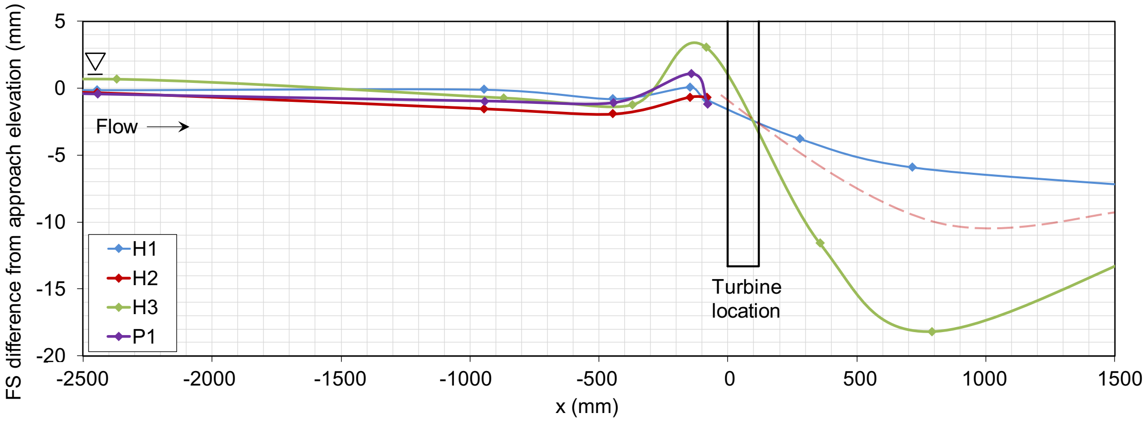

Fig. 7. Variation of flow free surface elevation along the flume at $t = 0$

4.4. Turbine tip-speed ratio (TSR)

The tip-speed ratio (TSR) of the turbine will determine the efficiency in producing electricity from the turbine. Although electricity production was not examined in this work, the effect of scour on TSR was investigated. TSR is defined as the ratio between the tangential speed of the tip of a blade and the flow velocity as following

$$\mathrm{TSR} = \frac{\omega \times \text{turbine radius}}{U}$$

where ω is the rotational speed of the turbine in rad/s, turbine radius is assumed 0.2m (see Fig. 2), and U is mean velocity of approach flow. Temporal variation of TSR is shown in Fig. 8. Dash lines show curves visually fitted to the data. In Run H3, the turbine blades were stationary and TSR = 0. Run P1 was also excluded since it was expected to have a similar rotational speed to Run H2. There are three findings from Fig. 8:

1. The turbine TSR progressively decreased with scour evolution. In 300 minutes, this reduction was 8% and 11% in Runs H1 and H2, respectively. It should be noted that the TSR is computed relative to the approach flow velocity U, which is constant since there has not been any scour upstream of the turbine.
2. The removal of the bottom plate in Run H2 reduced N by ~ 12% compared to Run H1, which is envisaged to be due to the enhancing effect of the bottom plate on the turbine performance. This highlights the importance of regular check-ups on the turbines to ensure that all structural components are accurately positioned and fully functional.
3. Rotational speed of the turbine in Run H1 continues to drop throughout the experiment, while in Run H2 it stabilizes after about 20 minutes. This is due to difference of scour depth, d_s, in Runs H1 and H2. In Run H2, smaller d_s is reached faster compared to Run H1 in which d_s takes longer to be attained.

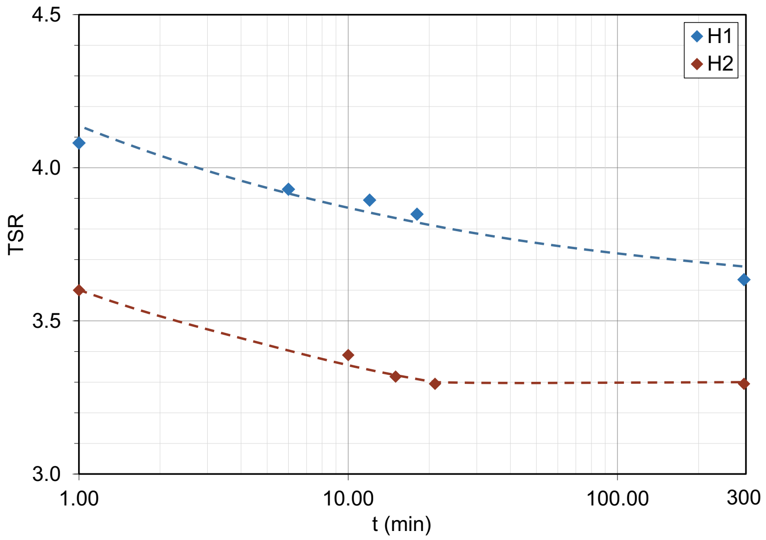

Fig. 8. Temporal variation of turbine TSR

5. Conclusions

This report presents findings from flume experiments on clear-water scour for a novel design of cross-flow turbine referred to as the MRL turbine. The main conclusions from this work are as follows.

1. The MRL turbine was found to produce significant downstream scour. The eroded sediment caused large deposition further downstream of the turbine which could have adverse impacts on the environment, navigation and habitat.
2. The scenario with the stationary turbine led to the largest scour. This is envisaged to be due to 1) special orientation of the blades, and 2) the turbine not spinning, both of which caused a large obstruction to the flow and directed all the flow energy toward eroding the sand bed. This result highlights the importance of continuously monitoring the turbine operation.
3. The turbine was found to run slower without the bottom plate, which is in agreement with previous findings in the literature (e.g. Gebreslassie 2012). This highlights the importance of regular inspection of the turbines to ensure all structural components are present and adequately secured.
4. Although the bottom plate was found to increase scour, it reduced flow free surface disturbance in the wake region of the turbine.
5. Temporal evolution of scour was found to reduce the rotational speed of the turbine, i.e. its efficiency in power production.
6. When the turbine was installed on piers (extended legs), it produced considerable local scour at the piers. The depth of scour at these locations could be even greater than the scour depth downstream of the turbine. This also needs regular monitoring to ensure stability of the turbine foundations.

Whilst these experiments have naturally been carried out for a specific (and novel) design of turbine, there is no reason to believe that such effects would not be at least as significant for any particular design of hydrokinetic turbine, leading the authors to emphasize the importance of further investigation of these scour effects.

Acknowledgements

The research presented in this paper was supported by funding from the UK's Engineering and Physical Sciences Research Council (EPSRC) under grant EP/M017354/1. Data supporting the presented work can be accessed via authors.

References

Chanson, H. (2004). *Hydraulics of Open Channel Flow*. Butterworth-Heinemann.
Elghali, S. E. B., Benbouzid, M. E. H., and Charpentier, J. F. (2007). "Marine Tidal Current Electric Power Generation Technology: State of the Art and Current Status." *2007 IEEE International Electric Machines Drives Conference*, 1407–1412.
Gebreslassie, M. G. (2012). "Simplified CFD modelling of tidal turbines for exploring arrays of devices." PhD thesis, Univeristy of Exeter.
Gebreslassie, M. G., Tabor, G. R., and Belmont, M. R. (2013a). "Numerical simulation of a new type of cross flow tidal turbine using OpenFOAM – Part I: Calibration of energy extraction." *Renewable Energy*, 50, 994–1004.
Gebreslassie, M. G., Tabor, G. R., and Belmont, M. R. (2013b). "Numerical simulation of a new type of cross flow tidal turbine using OpenFOAM – Part II: Investigation of turbine-to-turbine interaction." *Renewable Energy*, 50, 1005–1013.
Hill, C., Kozarek, J., Sotiropoulos, F., and Guala, M. (2016a). "Hydrodynamics and sediment transport in a meandering channel with a model axial-flow hydrokinetic turbine." *Water Resources Research*, 52(2), 860–879.
Hill, C., Musa, M., Chamorro, L. P., Ellis, C., and Guala, M. (2014). "Local Scour around a Model Hydrokinetic Turbine in an Erodible Channel." *Journal of Hydraulic Engineering*, 140(8), 04014037.
Hill, C., Musa, M., and Guala, M. (2016b). "Interaction between instream axial flow hydrokinetic turbines and uni-directional flow bedforms." *Renewable Energy*, 86, 409–421.
Janssen, A. P., and Belmont, M. R. (2009). *Initial research phase of MRL turbine. Technical Report No: MO 562L*. U.K.
Magagna, D., and Uihlein, A. (2015). "Ocean energy development in Europe: Current status and future perspectives." *International Journal of Marine Energy*, 11, 84–104.
Musa, M., Heisel, M., and Guala, M. (2018a). "Predictive model for local scour downstream of hydrokinetic turbines in erodible channels." *Physical Review Fluids*, 3(2), 024606.
Musa, M., Hill, C., Sotiropoulos, F., and Guala, M. (2018b). "Performance and resilience of hydrokinetic turbine arrays under large migrating fluvial bedforms." *Nature Energy*, 3, 839.
Ordonez-Sanchez, S., Sutherland, D., Payne, G. S., Bruce, T., Gebreslassie, M., Belmont, M. R., and Moon, I. (2017). "Experimental evaluation of the wake characteristics of cross flow turbine arrays." *Ocean Engineering*, 141, 215–226.
Sutherland, D., Ordonez-Sanchez, S., Belmont, M. R., Moon, I., Steynor, J., Davey, T., and Bruce, T. (2018). "Experimental optimisation of power for large arrays of cross-flow tidal turbines." *Renewable Energy*, 116, 685–696.
Wang, X., Wang, Z.-Y., Yu, M., and Li, D. (2001). "Velocity profile of sediment suspensions and comparison of log-law and wake-law." *Journal of Hydraulic Research*, 39(2), 211–217.
Yalin, M. S., and da Silva, A. M. F. (2001). *Fluvial processes*. IAHR, Delft.